Conversion of CO$_2$ over a Co-based Fischer-Tropsch catalyst

Debanjan Chakrabarti [a], Arno de Klerk [a *], Vinay Prasad [a],

Muthu Kumaran Gnanamani [b], Wilson D. Shafer [b], Gary Jacobs [b], Dennis E. Sparks [b],

Burtron H. Davis [b *]

[a] *Department of Chemical and Materials Engineering, University of Alberta, Edmonton, Alberta T6G 2V4, Canada.*

[b] *Center for Applied Energy Research, University of Kentucky, Lexington, KY, 40511, USA*

E-mail: deklerk@ualberta.ca; davis@caer.uky.edu

Abstract

The conversion of CO$_2$ over a CoPt/Al$_2$O$_3$ catalyst was investigated. Single gas adsorption studies indicated that carbon was deposited on the catalyst by exposure to both CO$_2$ and CO in the absence of H$_2$ co-feed. When CO$_2$ was pre-adsorbed followed by H$_2$ flow, methane was produced, as well as traces of C$_3$-C$_4$ hydrocarbons, but no evidence of the reverse water gas shift reaction was found. Use was made of carbon-14 labelled carbon dioxide to track CO$_2$ conversion and selectivity during reaction of syngas mixtures with different ratios of CO, CO$_2$ and H$_2$. Absence of ^{14}C in unconverted CO and the unequal molar concentration of ^{14}C in the products from reaction at 220 °C and 2 MPa provided strong evidence that ^{14}CO$_2$ was not converted by the reverse water gas shift reaction. The antecedence of the carbon from CO$_2$ mattered and the carbon did not become part of a common carbon pool for hydrocarbon synthesis. Conversion of CO$_2$ proceeded by a separate pathway from CO. Conclusions drawn from this experimental study were employed to point out implications for the industrial application of Co-catalysed Fischer–Tropsch synthesis.

Topical heading: Kinetics, Catalysis and Reaction Engineering.

Keywords: carbon dioxide, cobalt catalyst, Fischer–Tropsch, carburization, methanation, deactivation.

1. Introduction

Fischer–Tropsch (FT) synthesis involves the formation of a mixture of hydrocarbons, oxygenates and water, along with formation of carbon dioxide through the water gas shift reaction. The participation of carbon dioxide in the reaction network gives FT synthesis the potential to utilise CO_2 for the formation of useful products. However, to capitalise on this potential, or even to minimise CO_2 from the reaction system, it is essential to gain a proper understanding of the behaviour of CO_2 in the FT reaction. Various studies have been performed over the years to look into the mechanistic involvement of CO_2 on different FT catalysts.

Cobalt based catalysts generally have low water gas shift activity. On a cobalt catalyst, Riedel et al.[1] found CO_2 to behave as diluent for the CO and CO_2 did not affect the chain growth during FT synthesis, but CO_2 rather increased the methane selectivity. Over a 100 Co/60 MnO/147 SiO_2/0.15 Pt catalyst the methane selectivity increased from around 10 to 95 % as the CO_2 percentage of the CO_x content in the feed gas was increased for 0 to 100 %.[1] Analogous observations were reported for a 15 wt % Co on SiO_2 catalysts, with the methane selectivity changing from 10-15 to 75-85 % as the CO_x content of the feed gas was switched from CO to CO_2.[2] When co-feeding CO_2 an increase in methane selectivity was found for a Co supported on carbon nanofiber catalyst.[3] Increased methane production was also observed over a Co on thoria/magnesia-on-silica catalyst when the CO_2 content in the syngas was increased.[4] These observations suggest that the increase in methane selectivity when CO_2 is in the synthesis gas, is intrinsic to Co-FT catalysis and not the promoters or the support. It was further reported that the carbon number distribution of the heavier than C_2 products no longer followed an Anderson-Schulz-Flory (ASF) distribution.[1][2][5]

These observations suggested that CO_2 conversion took place independently from FT synthesis and that it provided a separate methanation pathway. It was proposed that the water gas shift reaction occurred on an oxide site, while chain growth occurred at a carbide site.[6] However, infrared spectroscopy studies by Visconti et al.[7] found that CO_2 and CO hydrogenation both proceeded via a common intermediate and they explained the different product trends by the difference in surface concentration ratio of carbon and hydrogen. It was further noted that

hydrogenation reactivity of CO_2 was higher than that of CO and that CO_2 hydrogenation had 90 % selectivity for methane.[7]

In this work, we explore the behaviour of CO_2 on a cobalt catalyst. The work was motivated by the need to better understand the conversion of CO_2 and its implications for the industrial application of Co-FT synthesis.

2. Experimental

2.1 Materials

The catalyst used for this study was 0.5 % Pt and 25 % Co on Al_2O_3. The catalyst was prepared using a sequential aqueous slurry impregnation method.[8] The catalyst was prepared with γ-Al_2O_3 support material (Condea Vista Catalox B: 100-200 mesh, 200 $m^2 \cdot g^{-1}$, pore volume 0.4 $cm^3 \cdot g^{-1}$). The support was calcined at 400 °C. Cobalt nitrate (>99.9 %, purity, supplied by Sigma Aldrich) was made into a slurry and impregnated onto the calcined support dropwise in three stages with vacuum evaporation step at 80 to 100 °C after each impregnation stage. Following the impregnation of the cobalt nitrate slurry, a similar impregnation step was carried out using a solution of tetraamine platinum (II) nitrate (>99.9 %, purity, supplied by Sigma Aldrich). Using a rotary evaporator, the catalyst was then dried under vacuum at 90 °C and then calcined at 350 °C for 4 hours under an atmosphere of air. The catalyst was analysed using a Micrometrics Tri-Star system and was found to have a BET surface area of 130 $m^2 \cdot g^{-1}$, pore volume of 0.282 $cm^3 \cdot g^{-1}$ and pore diameter of 1.91 nm.

Scott-Gross Company provided the CO, CO_2, H_2 and N_2 gases used for this study. The carbon-14 labelled barium carbonate ($Ba^{14}CO_3$) was supplied by American Radiolabeled Chemicals Inc. and had a specific activity of 1.85-2.22 $GBq \cdot mmol^{-1}$. The $Ba^{14}CO_3$ was used to synthesize $^{14}CO_2$.

2.2 Equipment and Procedure

The investigation comprised of two parts. The first series of experiments investigated the conversion of CO_2 and CO in the absence of a H_2 co-feed to study the persistency and reactions of the adsorbed gases. The second series of experiments made use of carbon-14 labelled CO_2 in syngas to study the effect of CO_2 incorporation in FT products.

Individually adsorbed CO and CO_2 conversion experiments

The experiments were conducted in a fixed bed reactor, length 50 cm and diameter 1.75 cm. The CO and H_2 flow were controlled using Brooks mass flow controllers. The CO_2 flow was controlled using an SFC2010 mass flow control valve by Semi Flow Engineering. The reactor was operated in down-flow mode and heated using a Lindberg Blue M tube furnace. The reactor was kept under isothermal conditions. The outlet of the reactor was connected to two 500 ml gas sample cylinders and then to a Swagelok back-pressure regulator. A HP Quad Series MicroGC Refinery Analyzer was then connected for performing gas analysis.

Blank runs were carried out using just glass beads (5 g) and no catalyst, to verify the inertness of the reactor system to the gases employed. The blank runs were conducted at 210 °C and 2 MPa absolute pressure. The first blank run checked for CO_2 conversion. After purging the system with N_2, the CO_2 was introduced. The gaseous product was analyzed after 1, 2 and 3 hours to check for any reactivity. The second blank run checked for H_2 and CO conversion. After purging the system with N_2, H_2 and CO were introduced into the system at H_2:CO molar ratio of 2. The product gas was analyzed after 1, 2 and 3 hours to check for any reactivity.

Three test runs were carried out (Table 1). In all three runs, 5 g of the catalyst was first reduced under an atmosphere containing H_2 and N_2 in the ratio 1:3, at 350 °C for 15 hours under atmospheric pressure. All gas volumes are reported as volumes at standard conditions. The reducing gas mixture was introduced into the system at a space velocity of 10 L·h^{-1}·(g catalyst)$^{-1}$. After reduction the temperature was decreased to 180 °C and the reactor was flushed with N_2 for 17 hours at 10 L·h^{-1}·(g catalyst)$^{-1}$ at atmospheric pressure to remove all H_2 in the system.

In Run 1, CO_2 was introduced into the system at a space velocity of 10 L·h^{-1}·(g catalyst)$^{-1}$ and the temperature and pressure in the reactor was increased to 210 °C and 2.0 MPa absolute pressure respectively. The system was left under this condition for 20 hours and it was then flushed with N_2 gas at 10 L·h^{-1}·(g catalyst)$^{-1}$ to remove CO_2 from the system and cooled to 22 °C. The system was depressurized under N_2 at 10 L·h^{-1}·(g catalyst)$^{-1}$ to release the adsorbed gases from the catalyst surface and the effluent was analyzed using the HP Quad Series MicroGC Refinery Analyzer. The spent catalyst was unloaded and analyzed. Carbon analysis was performed on the spent catalyst using a LecoCHN628 analyzer. Care was taken to ensure that the spent catalyst was not exposed to air. Before performing X-Ray Diffraction (XRD) analysis of the spent catalyst, the spent catalyst was first passivated overnight at room temperature by flowing a 1% O_2 in He mixture over the catalyst. The XRD analysis was performed using a Philips X'Pert diffractometer with monochromatic Cu Kα radiation.

In Run 2, the same procedure was followed but using CO instead of CO_2.

In Run 3, after reducing the catalyst and flushing out the reducing gas with N_2, the system was pressurized to 2.0 MPa absolute pressure by feeding CO_2 at a space velocity of 10 L·h^{-1}·(g catalyst)$^{-1}$ and the reactor temperature was increased to 210 °C. The system was left at this condition for 20 hours and then the system was flushed with N_2 for 24 hours at 10 L·h^{-1}·(g catalyst)$^{-1}$, and then depressurized quickly to remove some of the adsorbed CO_2. This was followed by flowing H_2 at atmospheric pressure for 24 hours at 10 L·h^{-1}·(g catalyst)$^{-1}$. The system was then again flushed with N_2 at 10 L·h^{-1}·(g catalyst)$^{-1}$ to remove H_2 from the system followed by flow of CO_2 at the same space velocity, 10 L·h^{-1}·(g catalyst)$^{-1}$. This cycle was repeated 2 more times, but with a lower inlet space velocity of H_2 of 1.4 L·h^{-1}·(g catalyst)$^{-1}$. In the third cycle, the H_2 was introduced into the system directly after Stage IV, without depressurizing the system under N_2 atmosphere to remove adsorbed CO_2. After 40 minutes of starting the H_2 flow under pressure, the system was depressurized quickly. Analysis of effluent gases was performed using gas chromatography after the system attained atmospheric pressure.

Carbon-14 labelled CO_2 co-feeding experiments

The experiments were conducted in a fixed bed reactor, length 17 cm and inside diameter 1.6 cm. The reactor was followed by a 500 ml hot trap kept at 170 °C and a 500 ml cold trap kept at 0 °C. A gas mixture (hereafter denoted as CO_{label}), 99.8% CO and 0.2 % $^{14}CO_2$ was prepared. For this gas mixture, the $^{14}CO_2$ was synthesized by titrating carbon-14 labelled $BaCO_3$ with H_2SO_4. The $^{14}CO_2$ so formed was transferred into a previously evacuated 5 L cylinder and was subsequently diluted with unlabeled CO.

For the experiment, 1.5 g of the catalyst was diluted with 9 g glass beads in the size range 40-100 μm. The catalyst was reduced in situ using a gas mixture of H_2 and N_2 mixed in the ratio of $H_2:N_2$ of 1:3 at 350 °C for 15 hours at atmospheric pressure. The system temperature was then decreased to 120 °C and syngas was introduced at $H_2:CO$ ratio of 3:1 at a flow rate of 9 standard $L \cdot h^{-1}$, i.e. a space velocity of 6 $L \cdot h^{-1} \cdot (g\ catalyst)^{-1}$. The system was pressurized to 2.0 MPa absolute pressure and the temperature was slowly increased to 220 °C in steps of 10 $°C \cdot h^{-1}$ to prevent temperature excursions in the reactor system.

Unlabeled syngas was initially used. The CO was then replaced with the CO_{label}. Unlabeled CO_2 was introduced to the system such that the total gas flow rate was unchanged and $H_2:(CO_{label} + CO) = 3$. Five different feed gas compositions (Table 2) were tested. In all of these experiments gas samples were taken only after six gas volume turnovers were completed.

The radioactivity in product fractions was determined by connecting a proportional counter in series with a gas chromatograph. This enabled the simultaneous measurement of concentration by the thermal conductivity detector and radioactivity by the proportional counter. The radioactivity of the product was determined by burning the effluent from the GC to CO_2. The radioactivity was proportional to the amount of ^{14}C. The threshold for naturally occurring background radioactivity was set at 100 counts per minute. Values below this threshold could not reliably be assigned to ^{14}C that originated from $^{14}CO_2$ in the feed gas. The limit of quantification for radioactive carbon is 1,500 counts per minute. This limit was set based on the signal-to-noise ratio.

3. Results and discussion

3.1 Blank runs

When CO_2 was fed to the reactor filled with glass beads, the product gas after 1, 2 and 3 hours on stream contained only CO_2. The N_2 used to initially purge the reactor was already completely displaced and no N_2 or CO was detected.

The blank run with CO and H_2 similarly yielded only CO and H_2 in the product. The product gas contained on average 33.6 ± 0.3 mol % CO and 65.0 ± 0.9 mol % H_2. No CO_2 and no CH_4 were detected in the product gas. The sample standard deviation provides an indication of the analytical variation inherent in the gas analysis and it gives and indication of the confidence in quantitative measurements.

The blank run tests confirmed the inertness of the reactor and glass beads with respect to the conversion of CO_2, CO and H_2.

3.2 CO_2 adsorption on catalyst

The procedure that was followed for adsorbing CO_2 on the catalyst is summarized as Run 1 in Table 1. When CO_2 was introduced into the system in Stage III of Run 1, trace amounts of H_2 were observed. In Stage V of Run 1, when the system was depressurized quickly under N_2, a significant concentration of CO_2 was observed in the effluent gas along with trace amounts of H_2 (Figure 1). There must have been sufficient unoccupied space available on the catalyst for CO_2 adsorption, because the amount of H_2 that was displaced was far less than the amount of CO_2 that was desorbed. No evidence of the reverse water gas shift reaction (Eq.1) was seen over the $CoPt/Al_2O_3$ catalyst.

$$CO + H_2O \rightleftharpoons CO_2 + H_2 \qquad \text{... (1)}$$

The carbon content of the spent catalyst was 3.8 wt %. The present work does not present further experimental evidence to distinguish between atomic carbon or carbon the form of a

carbide, only that carbon is present. The only carbon source was CO_2 and if carbon was deposited on the catalyst, the oxygen must have been rejected in some way. Some water may have been formed, but there was only a limited amount of H_2 on the catalyst. This implied that the catalyst was oxidized by the CO_2, since no other oxygen containing species were observed in the product gas. The catalyst consisted of the Fischer–Tropsch metal (Co), the reduction promotor (Pt) and the support (Al_2O_3) and of these it was most likely that it was the cobalt that was oxidized (Eq. 2).

$$CO_2 + 2 \, Co \; \rightarrow \; 2 \, CoO + C \qquad\qquad\qquad ... \,(2)$$

3.3 CO adsorption on catalyst

The procedure that was followed for adsorbing CO on the catalyst is summarized as Run 2 in Table 1. When CO was introduced into the system in Stage III of Run 2, CO_2 was observed in the effluent gas over an extended period of time (Figure 2). The formation of CO_2 was also accompanied by the presence of displaced H_2 from the catalyst surface, albeit at an order of magnitude lower concentration (Figure 2). No hydrocarbons were observed in the effluent gas.

It was unlikely that the bulk of the CO_2 observed could be produced by the water gas shift reaction (Eq. 1). The water gas shift reaction required water and there was no water in the feed gas. No Fischer–Tropsch hydrocarbon products were observed and there was no indication of CO hydrogenation to produce water. Furthermore, there was only a limited amount of H_2 adsorbed on the surface, some of which was displaced by CO by competitive adsorption. Since CO_2 continued to be produced as CO was introduced as feed gas (Figure 2), the CO_2 must have been produced by a different reaction. It is likely that the formation of CO_2 was due to a combination of the Boudouard reaction (Eq. 3) and the carburization reaction (Eq. 4) over the $CoPt/Al_2O_3$ catalyst.

$$2 \, CO \; \rightleftharpoons \; C + CO_2 \qquad\qquad\qquad ... \,(3)$$
$$2 \, CO + 2 \, Co \; \rightleftharpoons \; Co_2C + CO_2 \qquad\qquad\qquad ... \,(4)$$

The Boudouard reaction was reported before for Co-FT catalysts under H_2 starved operating conditions.[9][10]   Carburization of Co-FT catalysts has likewise been reported before.[11] Moodley[12] and Bartholomew[13] reviewed the different types of carbon deposits that are possible to from under typical FT conditions. On Ni-FT catalysts, carbon deposition under FT conditions was found to be a function of the partial pressure of CO.[12][14]   Surface carbide formed by dissociation of CO on the catalyst surface and carbon formation by the Boudouard reaction (Eq. 3) appear to be the most likely types of carbon deposits formed under the conditions of the present investigation. With prolonged exposure to CO it is also possible that polymeric carbon deposits were formed.

XRD analysis (Figure 3) of the spent catalyst revealed prominent peaks at around 43, 45-46 and 66-68 °, of which the peak at 42.6 ° was not only the most prominent, but also absent from the XRD pattern of the spent catalyst after Run 1 with just CO_2. Unfortunately the XRD analyses of the spent catalysts were inconclusive and the types of carbon deposits that were formed were not identified. The carbon content of the spent catalyst after treatment with CO was found to be 5.9 wt %, which was higher than the amount of carbon observed after CO_2 treatment. Cobalt is readily carburized by CO to form Co_2C, with free carbon being formed mainly at temperatures >225 °C.[11] Since the carbon content of the catalyst was higher than the stoichiometric amount required for conversion of Co to Co_2C (i.e. 2.3 wt % on a fresh catalyst basis containing 25 wt % Co), it was likely that at least some of this carbon was formed by the Boudouard reaction.

3.4 CO_2 adsorption followed by H_2

The effect of H_2 on a catalyst that was pre-adsorbed with CO_2 was investigated, as summarized in the procedure for Run 3 in Table 1. Three cycles of N_2 flushing, CO_2 adsorption, N_2 flushing and H_2 adsorption were performed.

In the first cycle when H_2 was introduced into the system in Stage VI of Run 3, the H_2 was introduced at a high space velocity, 10 $L \cdot h^{-1} \cdot$(g catalyst)$^{-1}$. Traces of methane and desorbed CO_2 were observed in the effluent gas for up to one hour. In the second cycle when H_2 was

introduced in Stage VI of Run 3, a lower space velocity was employed, 1.4 $L \cdot h^{-1} \cdot (g\ catalyst)^{-1}$. Methane and desorbed CO_2 was accompanied by trace amounts of C_3 and C_4 hydrocarbons in the product gas, but only for a short duration. In the third cycle, when H_2 was introduced into the system in Stage VI of Run 3, similar observations were made (Figure 4). Trace amounts of C_3 and C_4 hydrocarbons were observed when H_2 flow was introduced at high pressure, but only for a limited duration. When the system was depressurized under H_2 flow, trace amounts of C_3 and C_4 hydrocarbons were again observed.

The formation of methane (Figure 4) indicates that at least a part of the carbon present on the spent catalyst was not in the form of free carbon, because free carbon would require a higher temperature (>330 °C) to undergo methanation.[15][16] The results suggest that at least some of the carbon was present as a more easily reducible species, such as a surface carbide.

It has been observed that bulk carbides mainly have a tendency to participate in methanation.[9][10][17] Studies by Biloen et al.[18] reported significant incorporation of multiple carbon atoms from precarbided catalyst into the hydrocarbon chains of the products. They thus concluded that methanation and higher hydrocarbon product formation could occur from the same surface carbide intermediate.

The rate of carbide formation by a disproportionation reaction and the subsequent reduction of the carbides to hydrocarbons were reported.[15][16][19] These kinetic studies found that the rate of carbide formation by the disproportionation reaction was much slower than the rate of hydrogenation to hydrocarbons, and both these reactions were found to be slower than the rate of hydrocarbon formation by the FT synthesis. It was concluded that carbide formation via the carburization reaction could not be involved in creating the intermediate for FT reactions, but rather that FT synthesis could take place via hydrogen assisted carbide formation. However, on comparing the results from these kinetic studies,[15][16][19] with the results of Biloen et al.,[18] it could be inferred that the carbide formed via a disproportionation reaction can participate in hydrocarbon formation as well.

Since our studies found that CO_2 is capable of forming a reactive carbon species on the cobalt catalyst (Figure 4), two possibilities were considered:

(a) The CO_2 could be converted by the reverse water gas shift reaction with the adsorbed H_2 present on the catalyst surface to produce adsorbed CO. Visconti et al.[7] detected CO absorption by infrared spectroscopy when the feed gas contained CO_2 and H_2. Adsorbed CO could be readily converted to methane in the presence of the excess H_2 at Stage VI. However, there was no CO detected in the gas product even when the system was depressurized under N_2 in Stage V, while CO_2 was observed in the effluent gas (Figure 1). Also, in Stage III of Runs 1 and 3, when CO_2 was introduced into the system, the surface seemed to have an abundance of surface hydrogen. There was no methane or carbon monoxide detected in the effluent. No support was found in the present investigation that the reverse water gas shift reaction was active.

(b) The CO_2 could be dissociatively adsorbed to create a reactive carbon species, either by cleavage of one of the carbon-oxygen bonds (possibly assisted by surface hydrogen) to form a CH_xO intermediate,[2][8] or by dissociation of both carbon-oxygen bonds to form a surface carbide intermediate. Either of these surface species could be hydrogenated to methane. Biloen et al.[18] found that the carbide from the disproportionation reaction participated in hydrocarbon formation, which explained the trace amounts of C_3 and C_4 hydrocarbons that were observed (Figure 4). Results of $^{13}C^{18}O$ co-feeding experiments[20] have indicated that the formation of CO_2 may involve a cleavage of the carbon-oxygen bond first and then recombination of the carbon and oxygen species. By analogy the reverse reaction from CO_2 would also involve formation of an oxygen-free carbon species.

In conclusion, the experimental evidence pointed to the formation of a reactive surface carbon species by CO_2 over the $CoPt/Al_2O_3$ catalyst, which likely was cobalt carbide or analogous single carbon on cobalt species. However, considering the formation of C_{2+} hydrocarbons in a non-ASF profile,[5][7][21] under CO_2/H_2 feeding conditions, and the impact of co-feeding CO_2 with syngas on the methane formation,[1] the high methane selectivity still had to be explained.

It is speculated that due to the high local H_2 concentration on the surface, the carbide is mainly hydrogenated to methane. Chain growth could take place, but that chain growth was not based on average probability, but on local concentrations of active carbon species and hydrogen on the catalyst surface in the proximity of the surface carbide. This would explain the low selectivity to hydrocarbons, the prevalence of light hydrocarbons and the non-ASF carbon number distribution reported in literature.[5][7][21]

3.5 CO_2 and CO co-feeding at H_2:CO_x = 3:1

The experiments described previously considered the behavior of CO_x with no H_2 co-feed. In the next set of experiments, the behavior of CO_x was studied in a hydrogen-rich environment, with a constant H_2:CO_x molar feed ratio of 3:1. The objective of employing a high H_2:CO_x ratio was to encourage the reverse water gas shift reaction.

As a result of the high H_2:CO_x ratio, the amount of methane produced was high for all CO_x compositions tested (Table 3). As the fraction of CO_2 in the CO_x mixture was increased, the methane content of the gas phase product increased monotonically. The amount of liquid products that was collected was low and some liquid products were inevitably retained in the catalyst pores. The low amount of liquid product obtained made it difficult to reliably close material balances and the gas composition is therefore not expressed in terms of product selectivities. Conversion of CO cannot be inferred from Table 3. Nevertheless, useful observations about the conversion of the $^{14}CO_2$ that was present in the CO_{label} could still be made:

(a) The oil product that was obtained exhibited no radioactivity, which implied that little or no ^{14}C from $^{14}CO_2$ was incorporated into the heavier products from FT synthesis.

(b) The aqueous product contained only trace levels of alcohols. Like the oil product, the aqueous product exhibited no radioactivity.

(c) No radioactivity was found in the CO of the product gas.

(d) The gas phase products had different levels of ^{14}C incorporation from $^{14}CO_2$. Apart from CO_2, the only other products that exhibited radioactivity were the C_1-C_3 hydrocarbons. Multiple ^{14}C atoms were incorporated in C_2-C_3 molecules, i.e. ^{14}C was not just a chain initiator. The distribution of ^{14}C among the gas phase products is shown in Table 4. The conversion rate of $^{14}CO_2$ at 210 °C was in the range 1.3 to 3.4 $\mu mol \cdot s^{-1} \cdot (g\ catalyst)^{-1}$ for CO_2 partial pressures in the range 0.1 to 0.4 MPa. Note that the present investigation did not investigate or rule out carbon-isotope effects. The conversion of $^{14}CO_2$ is therefore not necessarily equivalent to the conversion of all CO_2 in the gas feed. Although direct comparison is not possible, Riedel et al.[1] reported a conversion rate of CO_2 at 190 °C in the range 0.3 to 1.3 $\mu mol \cdot s^{-1} \cdot (g\ catalyst)^{-1}$ for CO_2 partial pressures in the range 0.2 to 0.3 MPa.

(e) The CO_2 in a syngas feed that is passed over a $CoPt/Al_2O_3$ catalyst under FT synthesis condition is definitely not an inert and some of the CO_2 will be converted. This also holds true when the partial pressure of CO is much higher than that of CO_2.

(f) In the last run condition, $H_2:CO:CO_2 = 1:0:3$, the C_4 product exhibited a noticeable increase in branching compared to the C_4 products when CO was present in the feed gas.

The absence of ^{14}C in the CO remaining after reaction is noteworthy. The appearance of radioactive hydrocarbons without any radioactive CO could mean either of two possibilities. The first possibility is that hydrocarbon formation reactions are more rapid than desorption of CO formed by the reverse water gas shift reaction. As a result, any ^{14}CO formed from $^{14}CO_2$ reacts before desorption. If this is the case, then ^{14}C incorporation into the hydrocarbon products should be governed by reaction probability. The fraction of carbon that is ^{14}C should be similar for all carbon numbers, because FT chain growth does not depend on the antecedence of the CO. The second possibility is that the CO_2 is hydrogenated to form hydrocarbons by a pathway that is independent of FT synthesis based on CO hydrogenation and chain growth. If this is the case, then ^{14}C incorporation is likely to be restricted to light hydrocarbons, with the probability of chain growth being dependent on local H_2 concentration.

The abundance of ^{14}C in methane was in all instances higher than the calculated abundance that would have resulted if the probability of ^{14}C incorporation was based purely on the relative abundance of ^{14}C and independent of the antecedence of the ^{14}C (Figure 5). The calculated probabilities were restricted to the C_1-C_3 hydrocarbons. The difference between the calculated and observed values would have been larger if the full ASF distribution was considered. When antecedence does not matter and ^{14}C incorporation is based only on abundance, then the molar fraction of ^{14}C of the total C of each species should be the same.[22]

The restricted incorporation of ^{14}C in C_1-C_3 hydrocarbons (Table 4) and not in any heavier hydrocarbons, as well as the higher ^{14}C selectivity to methane (Figure 5), both supported an explanation based on CO_2 hydrogenation that is independent of normal FT synthesis. The antecedence of the ^{14}C mattered. The notion of carbon present in different adsorbed states on Co-FT catalysts is not a new concept. Different adsorbed states leading to different carbon pools being formed from CO over Co-FT was employed to explain different reaction pathways for methane formation.[23]

Moodley[12] discussed the possibility of multiple types of crystallographic sites on Co-FT catalysts. Some crystallographic sites were capable of causing CO dissociation, while other sites were capable of molecularly adsorbing CO. It was reported that there were cobalt surfaces where the CO dissociated to form Co_3C and no long chain hydrocarbons were adsorbed at these surfaces, but there were also other surfaces where CO dissociation appeared to favor long chain hydrocarbon growth.[12][24] Irrespective of whether the FT reaction follows a CO insertion mechanism, or a carbide mechanism, it is possible to envision a separate single carbon intermediate that may be responsible for a parallel reaction pathway.

The present experimental investigation showed that it is unlikely that CO_2 was converted by reverse water gas shift to produce a CO species that reacted in the same way as CO in the feed. The carbon from CO_2 did not enter a common carbon pool, but in some way retained a separate identity, which restricted its conversion to lighter products.

3.6 Role of alumina in the reaction chemistry

The catalyst support material for the Co-FT catalyst was alumina. The possibility that alumina contributed to the observed reaction chemistry, was considered. Alumina is active for both H and O exchange reactions at the temperature employed in this study (210 °C), including O exchange of CO_2.[25][26] Alumina has a rich surface chemistry, with at least seven different CO_2 adsorption modes being reported,[27] which explains the ease of oxygen exchange. However, CO_2 did not result in other products than oxygen exchanged CO_2. The site requirement for any type of hydrogenation on alumina is very demanding.[28] Hence, the contribution of the alumina support to the reactions observed in this study, if any, could be discounted.

3.7 Implications for industrial operation

There are three observations from the present investigation that have important implications for the industrial application of Co-FT synthesis. First, CO_2 is not inert during Co-FT synthesis and it is converted to mainly methane and other light hydrocarbon gases even at high H_2 and CO partial pressures.[1][2][3][4][5][7][21] Second, CO is susceptible to disproportionation over Co-FT catalysts and it can be a source of both carbon and CO_2. Third, CO_2 is also a potential source of carbon and a potential source of catalyst oxidation.

Although the experimental investigation did not attempt to mimic industrial operation, the observations indicated that CO_2 is not innocuous during Co-FT synthesis.

The presence of CO_2 in the feed to Co-FT synthesis is detrimental to the performance of the FT process. The CO_2 leads to methanation and a slight increase in light hydrocarbon gases. Neither is desirable during FT synthesis. In large-scale facilities a CO_2 removal step can be included in the gas loop design as part of the synthesis gas conditioning process before FT synthesis. For small-scale facilities, as is envisioned for the beneficiation of smaller unconnected natural gas deposits, there are additional design constraints to consider.[30] The inclusion of a CO_2 removal step will increase the complexity of the design. The added complexity of design, or alternatively the higher methane selectivity from Co-FT synthesis, detracts from the selection of Co-FT based synthesis gas conversion technology for small-scale gas-to-liquids facilities.

Disproportionation of CO is particularly detrimental to Co-FT synthesis. Although this is not a major reaction pathway, it is a source of CO_2 during Co-FT synthesis. Thus, even with a CO_2-free synthesis gas, the detrimental effects of CO_2 conversion by Co-FT cannot be completely avoided. Carbon formation has been implicated as a possible Co-FT catalyst deactivation mechanism.[10]

Carbon formation by either the Boudouard reaction (Eq. 3) or the carburization reaction (Eq. 4) produces CO_2 as a product. Subsequent hydrogenation of the carbon and the CO_2 can become an additional source of methane production during FT synthesis. It is speculated that the increase in methane selectivity over time as Co-FT catalyst deactivation progresses[31] might be related to the increased formation and subsequent hydrogenation of carbon and CO_2. An explanation based on increasing carbon formation and subsequent hydrogenation makes seems more plausible than attributing the increased methane selectivity of ageing Co-FT catalysts to an increase in CO hydrogenation activity. Carbon formation from CO_2 specifically, is insidious, because it can be accompanied by catalyst oxidation (Eq. 2). The oxidation of cobalt is also reported to be a cause of Co-FT catalyst deactivation, although water (not CO_2) is normally blamed for the oxidation leading to Co-FT catalyst deactivation.[32]

The effects of CO disproportionation and CO_2 derived carbon formation and catalyst oxidation will be exacerbated during process upset conditions that involve decreased H_2 partial pressure.

4. Conclusions

The behaviour of carbon dioxide and carbon monoxide was studied on a cobalt catalyst system under Fischer–Tropsch reaction conditions, but without hydrogen co-feed. The experimental results led to the following observations and conclusions:

(a) Carbon in some form was deposited on the $CoPt/Al_2O_3$ catalyst by exposure to both CO_2 and CO in the absence of hydrogen co-feed. More carbon was deposited due to exposure to CO than to CO_2. Carbon formation by CO_2 also implied some catalyst oxidation.

(b) When CO_2 was pre-adsorbed followed by the introduction of H_2, methane was produced, as well as traces of C_3-C_4 hydrocarbons. The experimental evidence pointed to the formation of a reactive surface carbon species on the $CoPt/Al_2O_3$ catalyst by CO_2. No evidence was found for the reverse water gas shift reaction to suggest that CO formed from the pre-adsorbed CO_2 when H_2 was introduced.

Following on the single gas experiments, the behaviour of different ratios of carbon dioxide and carbon monoxide was studied at a constant H_2:CO_x ratio of 3:1 under Fischer–Tropsch reaction conditions over a cobalt-based catalyst. Use was made of carbon-14 labelled CO_2 to identify the products derived from CO_2 during Fischer–Tropsch conversion. The experimental results supported the conclusions drawn based on the single gas experiments:

(c) The only products formed from $^{14}CO_2$ over the $CoPt/Al_2O_3$ catalyst were C_1-C_3 hydrocarbons, with methane being the dominant product. No ^{14}C was detected in the oil, aqueous product or unconverted CO. Furthermore, CO_2 was converted even when the CO and H_2 partial pressures were high.

(d) The absence of ^{14}C in unconverted CO and the unequal molar concentration of ^{14}C in the reaction products, provided strong evidence that CO_2 was not converted by the reverse water gas shift reaction to produce CO. The antecedence of the ^{14}C derived from $^{14}CO_2$ mattered. The carbon from CO_2 did not become part of a common carbon pool for reaction, but retained a different adsorbed identity and reacted by a different pathway from the main Fischer–Tropsch synthesis.

Acknowledgements

5. References

(1) Riedel, T.; Claeys, M.; Schulz, H.; Schaub, G.; Nam, S.-S.; Jun, K.-W.; Choi, M.-J.; Kishan, G.; Lee, K.-W., Comparative study of Fischer–Tropsch synthesis with H_2/CO and H_2/CO_2 syngas using Fe- and Co-based catalysts. *Appl. Catal. A* **1999**, *186*, 201-213.

(2) Zhang, Y.; Jacobs, G.; Sparks, D. E.; Dry, M. E.; Davis, B. H. CO and CO_2 hydrogenation study on supported cobalt Fischer–Tropsch synthesis catalysts. *Catal. Today* **2002**, *71*, 411-418.

(3) Díaz, J. A.; De la Osa, A. R.; Sánchez, P.; Romero, A.; Valverde, J. L. Influence of CO_2 co-feeding on Fischer–Tropsch fuels production over carbon nanofibers supported cobalt catalyst. *Catal. Comm.* **2014**, *44*, 57-61.

(4) Bessell, S. Cobalt based Fischer-Tropsch catalyst performance in the presence of nitrogen and carbon dioxide. *Stud. Surf. Sci. Catal.* **1994**, *81*, 483-486.

(5) Dorner, R. W.; Hardy D. R.; Williams, F. W.; Willauer, H. D. Heterogeneous catalytic CO_2 conversion to value-added hydrocarbons. *Energy Environ. Sci.* **2010**, *3*, 884-890.

(6) Van der Laan, G. P.; Beenackers, A. A. C. M. Kinetics and selectivity of the Fischer–Tropsch synthesis: A literature review. *Catal. Rev.-Sci. Eng.* **1999**, *41*, 255-318.

(7) Visconti, C. G.; Lietti, L.; Tronconi, E.; Forzatti, P.; Zennaro, R.; Finocchio, E. Fischer–Tropsch synthesis on a Co/Al_2O_3 catalyst with CO_2 containing syngas. *Appl. Catal. A* **2009**, *355*, 61-68.

(8) Gnanamani, M. K.; Jacobs, G. J.; Shafer, W. D.; Sparks, D.; Davis, B. H. Fischer–Tropsch synthesis: Deuterium kinetic isotope study for hydrogenation of carbon oxides over cobalt and iron catalysts. *Catal. Lett.* **2011**, *141*, 1420-1428.

(9) Weller, S. Kinetics of carbiding and hydrocarbon synthesis with cobalt Fischer–Tropsch catalysts. *J. Am. Chem. Soc.* **1947**, *69*, 2432-2436.

(10) Moodley, D. J.; Van de Loosdrecht, J.; Saib, A. M.; Niemantsverdriet, H. J. W. The formation and influence of carbon on cobalt-based Fischer–Tropsch synthesis catalysts. An integrated review. In *Advances in Fischer–Tropsch Synthesis, Catalysts and Catalysis*; Davis, B. H., Occelli, M. L. Eds.; CRC Press: Boca Raton, FL, **2010**, p 49-81.

(11) Hofer, L. J. E. Crystalline phases and their relation to Fischer–Tropsch catalysts. In *Catalysis Volume IV. Hydrocarbon synthesis, hydrogenation and cyclization*; Emmett, P. H. Ed.; Reinholt: New York, **1956**, p 373-441.

(12) Moodley, J. D. *On the deactivation of cobalt-based Fischer-Tropsch synthesis catalysts*; PhD thesis Technische Universiteit Eindhoven, Eindhoven, The Netherlands, 2008.

(13) Barthomolew, C. H. Carbon deposition in steam reforming and methanation. *Catal. Rev. – Sci. Eng.* **1982**, *24,* 67-112.

(14) Moeller, A. D.; Barthomolew, C. H. Deactivation by carbon of nickel, nickel-ruthenium and molybdenum methanation catalysts. *Ind. Eng. Chem. Process Des. Dev.* **1982**, *21*, 390-397.

(15) Craxford S. R. The Fischer–Tropsch synthesis of hydrocarbons, and some related reactions. *Trans. Faraday Soc.* **1939**, *35*, 946-958.

(16) Craxford S. R.; Rideal E. K. The mechanism of the synthesis of hydrocarbons from water gas. *J. Chem. Soc.* **1939**, 1604-1614.

(17) Kummer J. T.; De Witt T. W.; Emmett, P. H. Some mechanism studies on the Fischer–Tropsch synthesis using C^{14}. *J. Am. Chem. Soc.* **1948**, *70*, 3632-3643.

(18) Biloen P.; Helle J. N.; Sachtler W. M. H. Incorporation of surface carbon into hydrocarbons during Fischer–Tropsch synthesis: Mechanistic implications. *J. Catal.* **1979**, *58*, 95-107.

(19) Storch H. H.; Anderson R. B.; Hofer. L. J. E.; Hawk C. O.; Anderson H. C.; Golumbic N. Synthetic liquid fuels from hydrogenation of carbon monoxide; Technical Paper 709, U.S. Bureau of Mines, 1948.

(20) Chakrabarti D.; Gnanamani M. K.; Shafer W. D.; Ribeiro M. C.; Sparks D. E.; Prasad V.; De Klerk A.; Davis B. H. Fischer-Tropsch mechanism: Studies of a $Co/Ce_{0.75}Si_{0.25}$ catalyst using $^{13}C^{18}O$. *Prepr. Pap.-Am. Chem. Soc., Div. Energy Fuels* **2014**, *59* (2), 825-827.

(21) Dorner, R. W.; Hardy, D. R.; Williams, F. W.; Davis, B. H.; Willauer, H. D. Influence of gas feed composition and pressure on the catalytic conversion of CO_2 to hydrocarbons using a traditional cobalt-based Fischer-Tropsch catalyst. *Energy Fuels* **2009**, *23*, 4190-4195.

(22) Paál Z. Application of ^{14}C radiotracer for the study of heterogeneous catalytic reactions. In *Isotopes in heterogeneous catalysis*; Webb, G., Jackson, S. D., Hargreaves, J. S. J. Eds.; Imperial College Press: London, 2006, p 31-62.

(23) Yang, J.; Qi, Y.; Zhu, J.; Zhu, Y-A.; Chen, D.; Holmen, A. Reaction mechanism of CO activation and methane formation on Co Fischer–Tropsch catalyst: A combined DFT, transient, and steady-state kinetic modeling. *J. Catal.* **2013**, 308, 37-49.

(24) Geerlings, J. J. C.; Zonneville, M. C.; De Groot C. P. M. Fischer-Tropsch reaction on a cobalt (0001) single crystal. *Catal. Lett.,* **1990**, *5*, 309-314.

(25) De Klerk, A. Key catalyst types for the efficient refining of Fischer-Tropsch syncrude: alumina and phosphoric acid. In *Catalysis Vol. 23*; Spivey, J. J. , Dooley, K. M. Eds.; Royal Society of Chemistry: Cambridge, UK, 2011, p. 1-49.

(26) Peri, J. B. Oxygen exchange between $C^{18}O_2$ and "acidic" oxide and zeolite catalysts. *J. Phys. Chem.* **1975**, *79*, 1582-1588.

(27) Knözinger, H. Specific poisoning and characterization of catalytically active oxide surfaces. *Adv. Catal.* **1976**, *25*, 184-271.

(28) Hindin, S. G.; Weller, S. W. The effect of pretreatment on the activity of γ-alumina. I. Ethylene hydrogenation. *J. Phys. Chem.* **1956**, *60*, 1501-1506.

(29) Barrault, J.; Forquy, C.; Menezo, J. C.; Maurel, R. Hydrocondensation of CO_2 (CO), over supported iron catalysts. *React. Kinet. Catal. Lett.* **1981**, *17*, 373-378.

(30) De Klerk, A. Consider technology implications for small-scale Fischer-Tropsch GTL. *Gas Process.* **2014**, *July/August*, 41-48.

(31) De Klerk, A. Deactivation in Fischer-Tropsch synthesis and its impact on refinery design. *Prepr. Pap.-Am. Chem. Soc., Div. Petrol. Chem.* **2010**, *55* (1), 86-89.

(32) Tsakoumis, N. E.; Ronning, M.; Borg, O.; Rytter, E.; Holmen, A. Deactivation of cobalt based Fischer-Tropsch catalysts: A review. *Catal. Today* **2010**, *154*, 162-182.

Table 1. Operating conditions for individually adsorbed CO and CO_2 conversion experiments.

Run	Stage I	Stage II	Stage III	Stage IV	Stage V	Stage VI
Run 1	Feed = H_2:N_2 (1:3)	Feed = N_2	Feed = CO_2	Feed = N_2	Feed = N_2	
	T = 350 °C	T = 180 °C	T = 210 °C	T = 22 °C	T = 22 °C	
	P = 0.1 MPa	P = 0.1 MPa	P = 2.0 MPa	P = 2.0 MPa	P = 0.1 MPa	
	Time = 15 h	Time = 17 h	Time = 20 h	Time = 24 h	Time = 24 h	
Run 2	Feed = H_2:N_2 (1:3)	Feed = N_2	Feed = CO	Feed = N_2	Feed = N_2	
	T = 350 °C	T = 180 °C	T = 210 °C	T = 22 °C	T = 22 °C	
	P = 0.1 MPa	P = 0.1 MPa	P = 2.0 MPa	P = 2.0 MPa	P = 0.1 MPa	
	Time = 15 h	Time = 17 h	Time = 20 h	Time = 24 h	Time = 24 h	
Run 3[a]		(start of cycle)				(end of cycle)
	Feed = H_2:N_2 (1:3)	Feed = N_2	Feed = CO_2	Feed = N_2	Feed = N_2	Feed = H_2
	T = 350 °C	T = 180 °C	T = 210 °C	T = 210 °C	T = 210 °C	T = 210 °C
	P = 0.1 MPa	P = 0.1 MPa	P = 2.0 MPa	P = 2.0 MPa	P = 0.1 MPa	P = 0.1 MPa
	Time = 15 h	Time = 17 h	Time = 20 h	Time = 24 h	Time = 24 h	Time = 24 h

[a] Cycle was repeated three times, with modifications as indicated in the text.

Table 2. Feed compositions for CO_2 co-feeding experiments

Condition	H_2	CO_{label} [a]	CO_2
I	3	1	0
II	3	0.75	0.25
III	3	0.50	0.50
IV	3	0.25	0.75
V	3	0	1

[a] CO_{label} = 99.8% CO and 0.2 % $^{14}CO_2$

Table 3. Gas phase composition from the conversion of H_2, CO and CO_2 mixtures over CoPt/Al_2O_3 at 220 °C, 2.0 MPa and constant volumetric flow rate.

Feed gas H_2:CO:CO_2	space velocity, $L·h^{-1}·(g\ catalyst)^{-1}$	Gas phase product, mol % [a]								
		CO	CO_2	CH_4	C_2	C_3	C_4	C_5-C_6	H_2O [b]	H_2 [c]
3 : 1 : 0	6	17.9	0.6	4.9	0.2	0.3	0.3	0	0.6	75.1
3 : 0.75 : 0.25	6	10.4	11.0	6.9	0.2	0.3	0.2	0	0.6	70.2
3 : 0.5 : 0.5	6	3.8	18.5	11.1	0.3	0.3	0.2	0	0.6	65.1
3 : 0.25 : 0.75	6	0	23.1	16.9	0.4	0.4	0.1	0	0.6	58.6
3 : 0 : 1	6	0	28.2	19.6	0.4	0.5	0.1	0.1	0.6	50.5

[a] Liquid products excluded; these results do not reflect the material balance.

[b] Based on water partial pressure at cold product knockout conditions, not directly measured.

[c] Calculated based on difference.

Table 4. Conversion of $^{14}CO_2$ and selectivity of ^{14}C in products during the conversion of H_2, CO and CO_2 mixtures over $CoPt/Al_2O_3$ at 220 °C and 2.0 MPa.

Feed gas [a]	$^{14}CO_2$ conversion	^{14}C selectivity		
H_2:CO:CO_2	(%)	CH_4	C_2	C_3
3 : 1 : 0	33	94	4	2
3 : 0.75 : 0.25	28	90	4	6
3 : 0.5 : 0.5	37	97	3	0 [b]
3 : 0.25 : 0.75	20	96	4	0 [b]

[a] The $^{14}CO_2$ was introduced as CO_{label} and the H_2:CO:CO_2 = 3:0:1 feed did not contain $^{14}CO_2$.

[b] If any ^{14}C was incorporated the selectivity was 0.1 % or less.
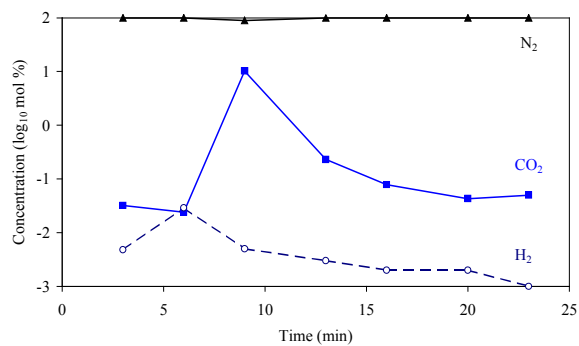
Figure 1. Gas composition over time as CO_2 treated $CoPt/Al_2O_3$ catalyst was depressurized under N_2 flow (Run 1, Stage V). Gases shown are N_2 (▲), CO_2 (■) and H_2 (○). Time = 0 min represents the time at which the system was depressurized.
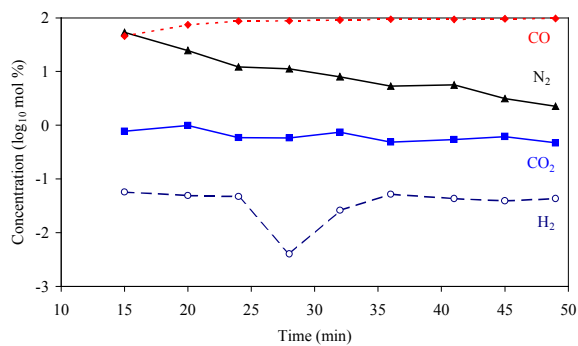
Figure 2. Gas composition over time as CO was introduced as only feed over CoPt/Al_2O_3 at 210 °C and 2.0 MPa (Run 2, Stage III). Gases shown are N_2 (▲), CO_2 (■), CO (♦) and H_2 (○). Time = 0 min represents the time at which CO was introduced into the system.
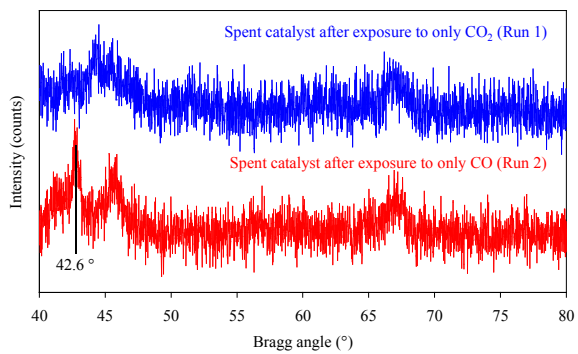
Figure 3. XRD analyses of spent CoPt/Al$_2$O$_3$ catalysts after treatment with only CO$_2$ (Run 1) and only CO (Run 2).
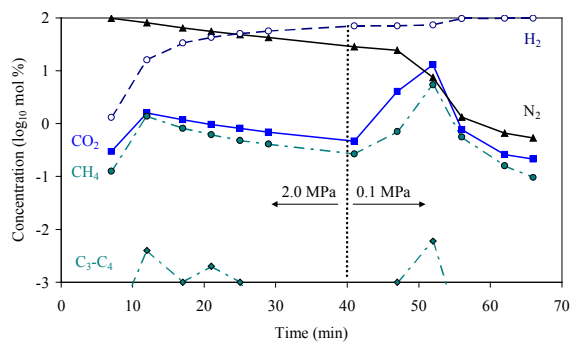
Figure 4. Gas composition over time as H_2 was introduced after CO_2 adsorption on CoPt/Al_2O_3 during the third cycle of Run 3 at Stage VI. Time = 0 min represents the time at which H_2 was introduced to the system. Quick depressurization was achieved at time = 57 min.
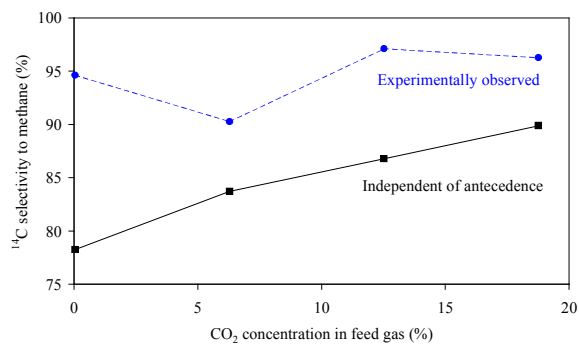
Figure 5. Observed selectivity of ^{14}C incorporation in methane (●), compared to abundance based ^{14}C incorporation in methane (■), when incorporation is restricted to C_1-C_3 hydrocarbons and independent of ^{14}C antecedence.